ASE- 3857

FINAL REPORT

Contract NASW-2292 Phases II, III and IV

FABRICATION OF A FOCUSING SOFT X-RAY COLLECTOR PAYLOAD

30 June 1976

Prepared by:

J. M. Davis, A.R. DeCaprio, H. Manko , J.W.S. Ting

American Science and Engineering, Inc.
955 Massachusetts Avenue
Cambridge, Massachusetts 02139

Prepared for:

Goddard Space Flight Center
National Aeronautics and Space Administration
Greenbelt, Maryland 20771

Period of Performance:

22 November 1972 to 30 June 1976

Approved by:

John M. Davis

John M. Davis
Program Manager

FOREWORD

This document is the Final Report for Phases II, III and IV for NASA Contract NASW-2292. The period of performance for the three phases was 22 November, 1972 to 31 January 1976. The contract provided for the fabrication of a soft x-ray collector payload and for its launch on Aerobee 350 sounding rockets 17.015UG and 17.016UH.

Note: Following the flight of 17.016UH the contract was extended, at no increase in cost, until June 30, 1976 in order to allow AS&E to support the refurbishment and flight of 17.017UH. The launch took place on the night of June 16, 1976. The instrument functioned normally during the flight and was recovered intact.

CONTENTS

LIST OF ILLUSTRATIONS

List of Tables

1.0 INTRODUCTION

1.1 Background

Following the discovery of stellar x-ray sources, the science of x-ray astronomy has developed rapidly as increasingly sophisticated measurement techniques have provided new information on source positions, the time variations of the radiation and its spectral and spatial distribution. For the class of x-ray objects which possess a finite size, when viewed from the earth, two-dimensional images would provide significant information on the precise source position and the spatial distribution of the emitting material. To achieve these goals a program of focusing stellar x-ray astronomy was initiated, with NASA support, at AS&E. One phase of the program was aimed at the development of large area imaging system capable of operation from sounding rockets. It was initiated in 1969, under the direction of Dr. Paul Gorenstein, with the issuing of NASA contract NASW-1889 and has continued through the present under NASA contract NASW-2292. During the performance of the first contract, a one-dimensional focusing instrument was developed and flown. Contract NASW-2292 was granted to re-fly (Phase I), improve the instrument (Phase II) and obtain new flight data (Phases III and IV). Halfway through the performance of Phase II, the scientists, including the Principal Investigator, associated with the program, transferred their affiliation from AS&E to the Smithsonian Astrophysical Observatory, Cambridge, Massachusetts (SAO). At this time, June 1973, the responsibility for the tasks described in the statement of work of Contract NASW-2292 were divided between the two institutions. SAO was responsible for the analysis of the data from the flight undertaken during Phase I and for the overall scientific direction of the Program. AS&E was responsible for the design and fabrication of the new payload and for integration and launch support.

This report covers the work performed by AS&E under Phases II, III and IV of NASA contract NASW-2292 and covering the period of performance from 31 September, 1972 to 31 January, 1976.

1.2 X-Ray Imaging

The application of focusing x-ray optics to stellar astronomy was first discussed by Giacconi and Rossi (1960). They described an optical system which would focus x-rays using the principle of total external reflection for glancing incidence rays. Wolter (1952 a, b) had shown that reflections from two successive conic sections are required to minimize the optical aberrations of the system. This principle, when used with paraboloid-hyperboloid combinations has been highly successful in obtaining high resolution (1-2 arc second) images of the solar x-ray corona (Vaiana, 1972). However the application of this type of system to stellar astronomy is limited because the reflecting surfaces tend to have small collecting areas and the stellar sources have low flux levels. Consequently the amount of observing time provided by a sounding rocket flight is insufficient to accumulate enough data for reasonable images.

It was soon realized that x-ray mirrors with much greater collecting areas can be constructed using a design concept first suggested by Kirkpatrick and Baez (1948) of crossed spherical reflectors. A simplified Kirkpatrick-Baez device is shown in Figure 1-1 (a). The incident ray strikes successively two paraboloids oriented perpendicularly to one another. In practical designs, the surface area is increased by using many approximately parallel paraboloids. Figure 1-1 (b).

The first test of this design took place in June 1970, when a one-dimensional array was flown aboard an Aerobee 170 rocket to observe portions of the constellations Virgo and Cygnus (Gorenstein et. al., 1971). The flight was successful and the instrument was

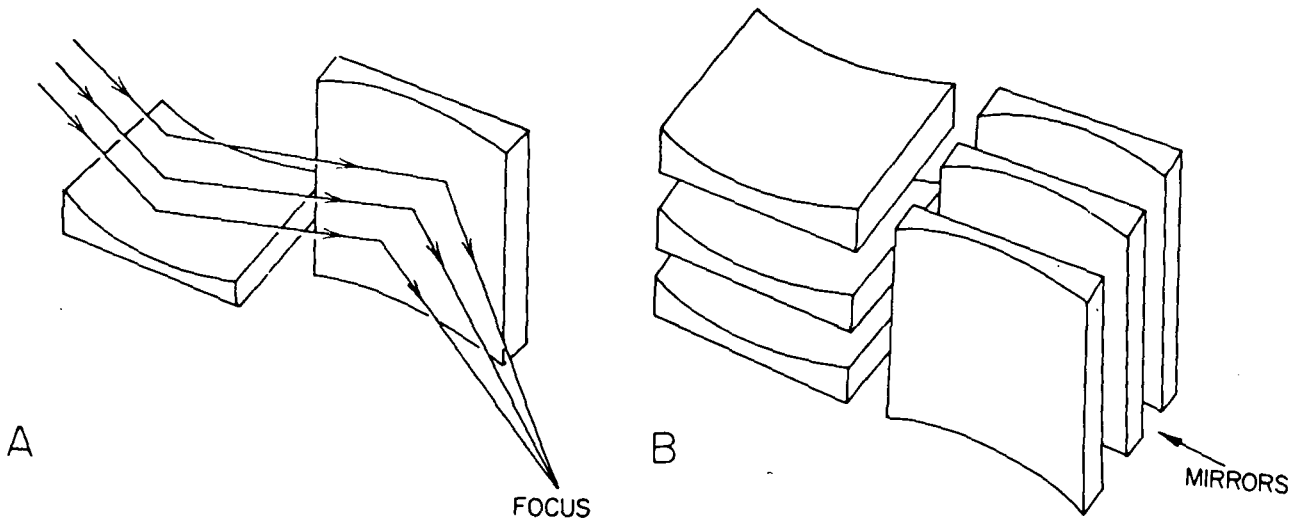

Figure 1-1. (A) A Simple Kirkpatrick-Baez Device.
(B) A Nested Set of Orthogonal Mirrors.

improved and reflown in April, 1972, under Phase I of this contract, to study the Vela-Puppis region (Gorenstein et. al., 1973). Following the flight it was felt that sufficient practical experience had been gained with the one-dimensional system to start development of a true two-dimensional imaging system. In the following sections the design, fabrication and testing of the two-dimensional mirror and payload will be described.

1.3 Electronic Image Detection

Stellar x-ray sources have relatively low flux levels, consequently the traditional image recording methods (e.g. photographic film) are too insensitive and it is necessary to turn to electronic imaging techniques, with which the individual x-ray photons are detected and recorded. Two different approaches to electronic imaging appeared technologically feasible at the start of the program. Both rely on the conversion of the incident photon into an electron and its subsequent amplification. In the first technique, the micro-channel plate, the spatial location of the incident photon is retained by allowing the electron amplification to occur within one of an array of small tubelets across which an electric potential has been applied. The resulting electron beam can be detected by a variety of techniques e.g. proximity focusing onto a phosphor screen coupled to a TV camera. This method is useful for high resolution (arc second), small field of view (1 square degree) applications. However the objectives of the present experiment called for a large field of view instrument with only moderate resolution (arc minutes) and a large field of view (10 square degrees) and the Imaging Proportional Counter (IPC) approach was chosen. With this detector the location of the electron avalanche occurring at the anode wire is measured. Since the IPC still retains the properties of a traditional proportional counter it possesses the additional

advantage of being able to measure the energy of the incident photon, thus permitting spectral measurements to be made at each spatial location.

IPC's are multiwire proportional counters in which the anode plane is situated between two cathode planes. The latter are each formed from a continuous wire which is wound in such a way as to map the plane in one-dimension (Figure 1-2). The avalanches arising from x-ray events occur in the proximity of an anode wire and the motion of the positive ions in the large electric fields at the vicinity of the wires induces fast-rising positive pulses on the surrounding cathodes. Different methods have been developed to determine the position of the centre of the avalanches. The most common are the delay-line method of the Perez-Mendez Group (Perez-Mendez, 1974), the rise-time method of Borkowski and Kopp (1972) and a center of gravity analysis of groups of cathode wires (Charpak, 1974).

Following a review of the possible techniques it was decided to adopt the approach of Borkowski and Kopp and to attempt to extend their results to lower photon energies.

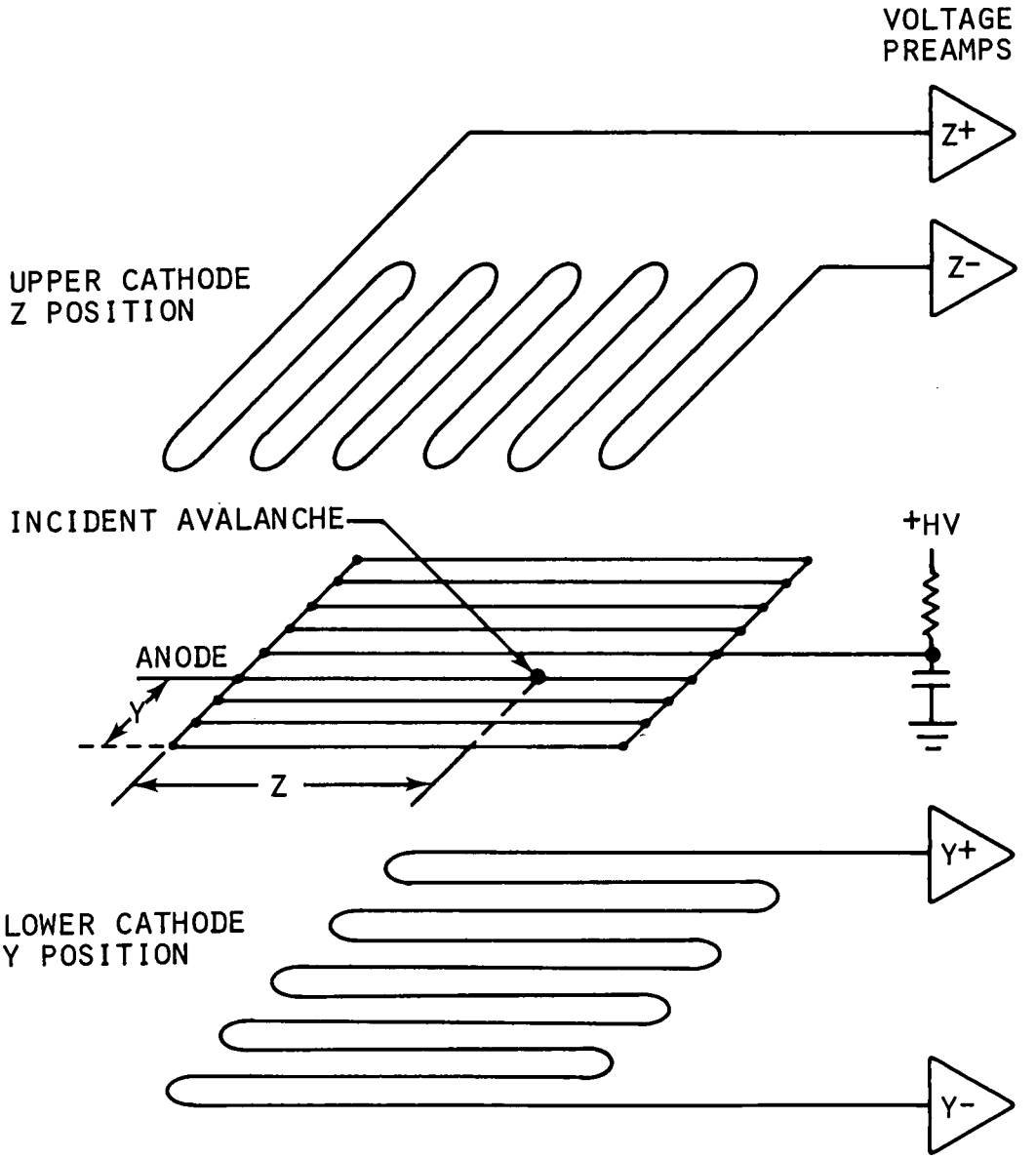

Figure 1-2. Simplified Diagram of the Electrode Arrangement Within an Imaging Proportional Counter

2.0 THE TWO-DIMENSIONAL FOCUSING PAYLOAD

2.1 General

Figure 2-1 shows a schematic representation of the payload. It consists of

(a) The two-dimensional crossed paraboloid mirror assembly.

(b) An aspect camera and star tracker

(c) A focal plane assembly containing an imaging proportional counter and its preamplifiers, high voltage power supplies and gas system.

(d) A fiducial system

(e) Housekeeping, data handling, instrumentation and telemetry electronics.

The primary design criterion was to build a mirror with sufficient collecting area to ensure adequate counting statistics. For this reason an Aerobee 350 was chosen for the launch vehicle which provided a payload cylinder of diameter 55.9cm and length 254 cm. To conserve cost the fabrication of the basic structure was undertaken by GSFC to the design developed by AS&E . The fabrication was subcontracted by GSFC to the Middlestadt Machine Company of Baltimore, Maryland.

2.2 The X-Ray Mirror

The general geometric relations governing nested arrays of orthogonal parabolas have been derived by Van Speybroeck et.al., (1971) and their equations were used to develop the design parameters of the mirror. In general the parameters can be restricted to the effective diameter of the mirror, the length of the reflecting surfaces, the focal lengths of the mirrors and the orientation of the individual plates to the central axis. As these parameters are varied the resolution and collecting area are determined using ray tracing techniques for each configuration. For radiation on-axis the resolu-

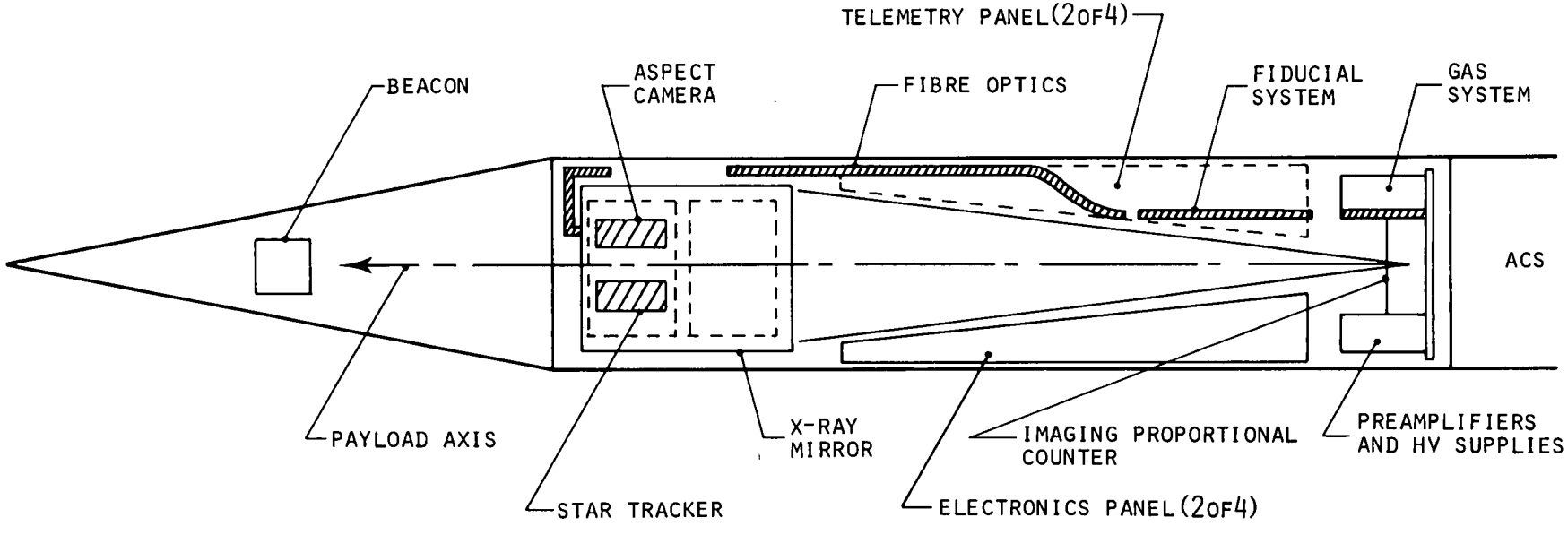

Figure 2-1. Schematic Diagram of the Aerobee 350 Payload

tion is theoretically perfect in one-dimension and about a second of arc in the orthogonal direction. Off-axis the resolution degrades as the first power of the angle. In practice, alignment errors and imperfections in the reflecting surfaces have limited the resolution to a few arc minutes everywhere within the field of view.

Table I summarizes the characteristics of the telescope. The effective collecting area has been determined by ray tracing using the values of the x-ray reflectivity as a function of angle of incidence measured during Phase I of this contract.

2.2.1 Material

The reflecting surfaces consist of commercially available float glass coated with 500 Å of gold upon a 500Å chromium base. This is the same material used for the one-dimensional collectors and it was chosen because of the following factors.

(a) Adequate reflectivity and scattering properties over the range of wavelengths and incident angles required.

(b) Good physical stability for maintaining the desired curvature under stress.

(c) Relatively low cost and good availability compared to polished surface materials.

2.2.2 Assembly and Alignment

The mechanical design of the mirror must satisfy certain criteria. Briefly they are

(a) It must provide a method of achieving the desired curve on each of the mirror surfaces.

(b) It must allow the images from the separate surfaces to be superimposed.

(c) It must maintain the geometrical relations between the surfaces and ensure their survival through the full range of environments associated with a sounding rocket flight.

TABLE 1

CHARACTERISTICS OF LARGE AREA FOCUSING COLLECTOR FOR AEROBEE 350

Focal Length	180 cm
Number of Plates	26 Front (25.4cm x 50.8cm x .25cm) 18 Rear (36.8cm x 50.8cm x .25cm)
Total Geometric Area	40.6 x 25.4 ~ 1000cm^2
Effective Area of Assembly	185cm^2 (θ = 0, λ = 10 Å) 264cm^2 (θ = 0, λ = 44 Å)
Detector Efficiency	.65 (λ=10 Å) .55 (λ = 44 Å)
Net Effective Area	120cm^2 (θ = 0, λ=10 Å) 145cm^2 (θ = 0, λ=44 Å)
Field of View	40 arc minutes, radius, FWHM
Angular Resolution	3 arc min x 3 arc min Design 1 arc min x 1 arc min Achieved

Our approach has been to mount the plates within a rectangular aluminum sheet metal box which is supported at each end by relatively massive magnesium plates. The plates are held together by longerons which provide torsional stiffness to the assembly and also allow for mounting points to the payload structure (Figure 2-2a).The longerons are also useful in adjusting the separation of the two mirror assemblies for the best focus. A photograph of the assembled mirror is shown in Figure 2-2b .It is 101.6cm long and weighs approximately 528 kg. and is positioned in the payload structure through a system of 24 Barry isolation mounts. The system has proved effective against misalignments arising during the powered phase of the rocket flight. Tests performed after recovery have shown no evidence of degradation of the mirror images.

The isolation system has also proved to be effective in stabilizing the payload when subjected to the Aerobee vibration and acceleration test levels. After a typical series of vibration tests the change in relative alignment between the optic axis of the mirror assembly and a fixed point in the focal plane was less than 10 minutes of arc. The change in internal alignment of the mirror assembly i.e. the change in relative position of the images from different surfaces, was less than 20 arc seconds.

The individual glass plates are bonded to aluminum channels which in turn are mounted within the rectangular box container. The aluminum channels run the full length of the plates and care was taken during the bonding process to ensure a uniform separation between the channels along their entire length. Mylar adhesive tape (.005 cm thick) was attached to the back of the plates to retain the glass in the event of fracturing. To complete the mirror aperture plates of 0.018cm aluminum foil were formed and bonded

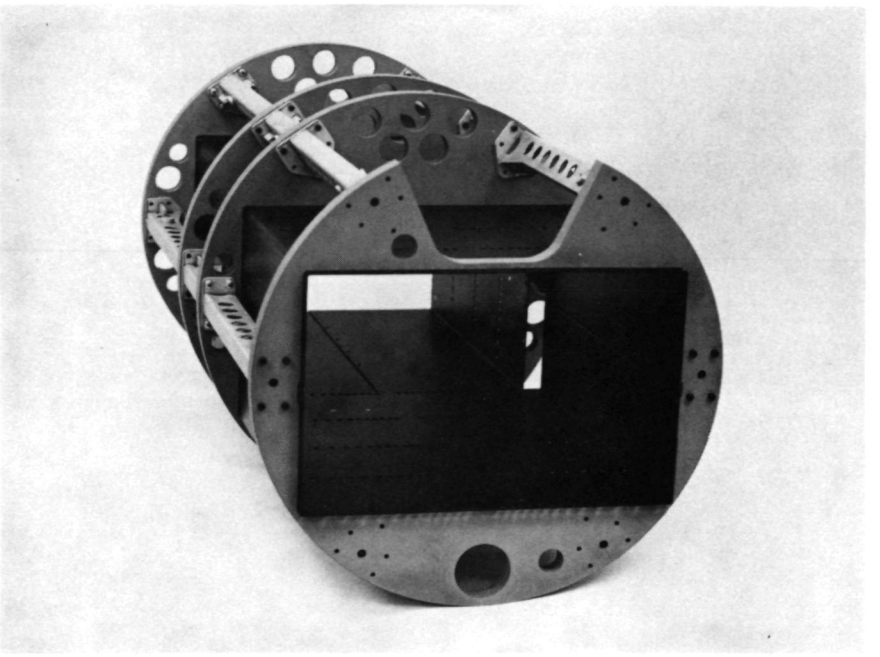

EW-013

(a)

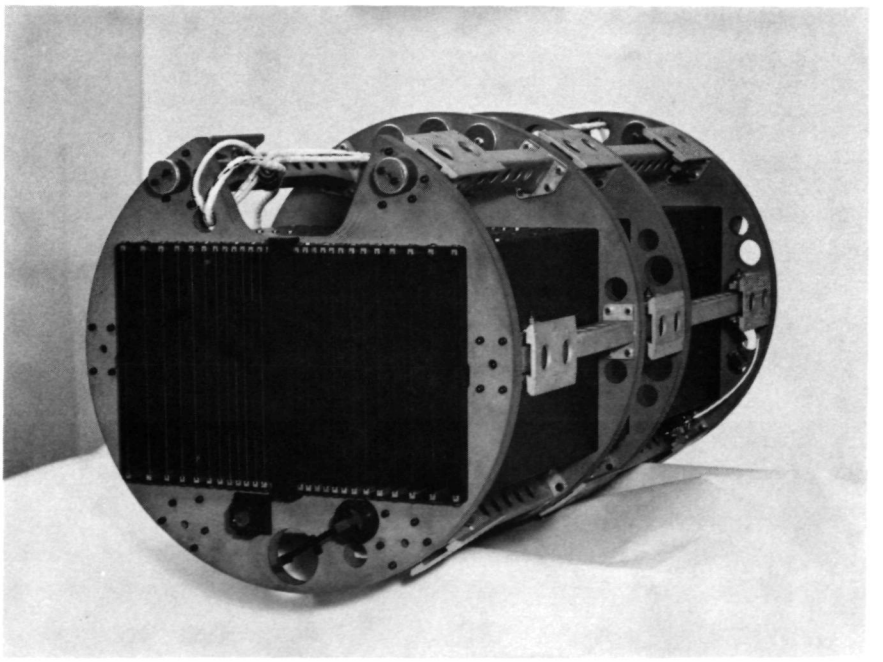

EW-045

(b)

Figure 2-2. (a) The X-ray Mirror Assembly Showing the Sheet Metal Mounting Box, Longerons, and End Plates

(b) The Fully Assembled Mirror

to the rear of each plate to eliminate straight through radiation i.e. incident x-rays which had passed through the mirror without suffering reflection .

The mirror surfaces are held in position by attaching the aluminum channels to the rectangular box at 5 points along the nominal parabolic curve with eccentric bushings having screws in an axis hole for clamping purposes. Each bushing can be displaced independently about 0.25mm and is clamped by the screw prior to being expoxied in its desired location.

To align the plates, the individual mirror assemblies are set on an optical bench and illuminated with collimated light from a point source. In the focal plane the image from a single surface will be spread out into a line. The first stage in the procedure is to superimpose the images from the different plates by manually 'tuning' the curve of each reflecting surface. The effect of the tuning is observed by placing slits in the focal plane near to both extremities of the image. Photoelectric detectors are mounted behind the slits and the curve of the plate adjusted until the output of the detector is maximized.

The above procedure is complicated by synclastic bending. This effect introduces a curvature in an orthogonal direction when the glass is bent to conform to the desired arc. (See Figure 2-3 for a schematic representation). The result of the synclastic bending on the image is a bending and spreading of the line image primarily at its ends (Figure 2-3b). If the synclastic effect is tuned out the resulting image shows marked improvement.

After both sets of mirrors have been aligned they are mounted together and the combined image can be observed. For test purposes we have used a star pattern, which has 30 arc second

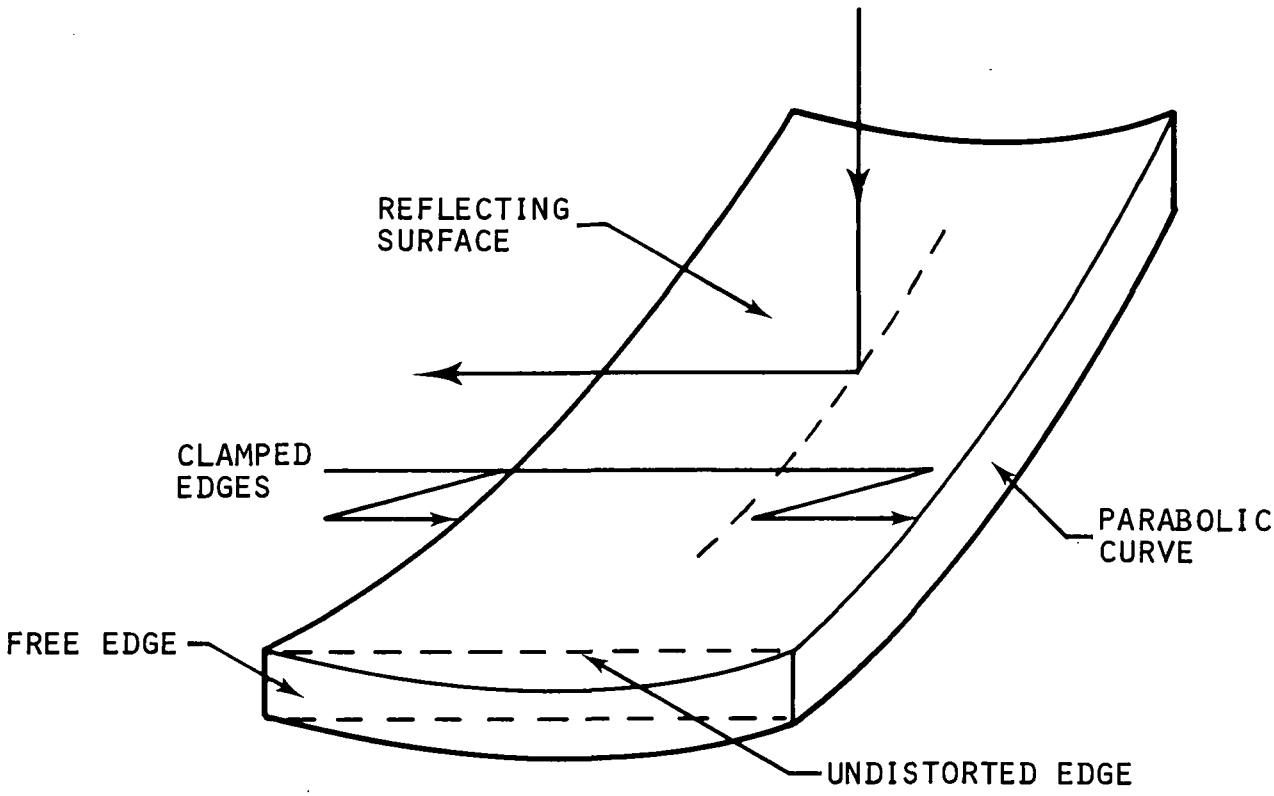

Figure 2-3. (a) Schematic of a Mirror Plate Showing the Distortion Produced Along the Free Edges When the Clamped Edges are Bent Into a Parabola.

Figure 2-3. (b) Diagram of a Line Image From a Single Reflection Showing the End Spreading Due to the Synclastic Bending.

pinholes on 3.3 arc minute centers. Two sets of images are shown in Figures 2-4 and 2-5. The test plates were taken before the first and second flights respectively and the improvement in the second set of images is due almost entirely to the removal of the synclastic effect. For these images the resolution approaches one minute of arc. To reach this level it was necessary to repeat the tuning procedure several times, at each stage making slight improvements to the one-dimensional image.

2.2.3 The Fiducial System

The mirror assembly is attached to the structure through the vibration isolation system. This does permit slight motion of the assembly with respect to the structure and in order to correct for possible changes in alignment, during flight, a fiducial light system is used to mark the position of fixed points in the focal plane relative to the mirror system. The information is transmitted to the aspect camera by means of relay lenses, prisms and a fiber optics light guide (Figure 2-6). In operation a pinhole array is attached to the counter body and is imaged through two lenses onto a coherent fiber bundle attached directly to the mirror assembly. The exit of the fiber bundle is viewed by a collimating lens which relays the light beam to the star camera.

Changes in alignment between the counter and mirror will alter the position of the pinhole array in the aspect camera field. The range of the fiducial system and the focal plane coverage of the detector is far greater than any expected or experienced changes in the alignment.

2.2.4 Mechanical Drawings

A complete set of engineering drawings for the payload structure and internal components was made during the design and fabrication phases of the contract. Although not included in this report they are available upon request.

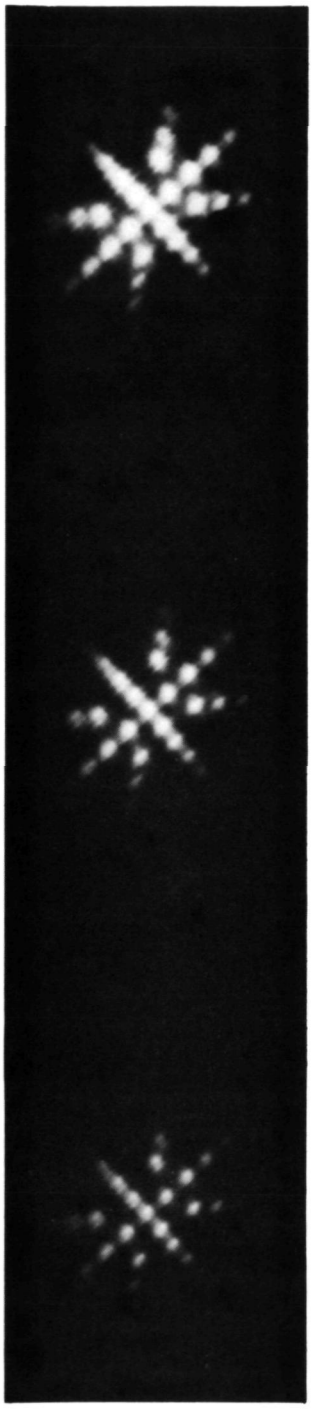

Figure 2-4. A Pinhole Array Photographed with the Two Dimensional Focusing Collector Prior to the First Flight. The Pinholes Have an Angular Diameter of 30 Arc Seconds and a Center to Center Separation of 3.3 Arc Minutes

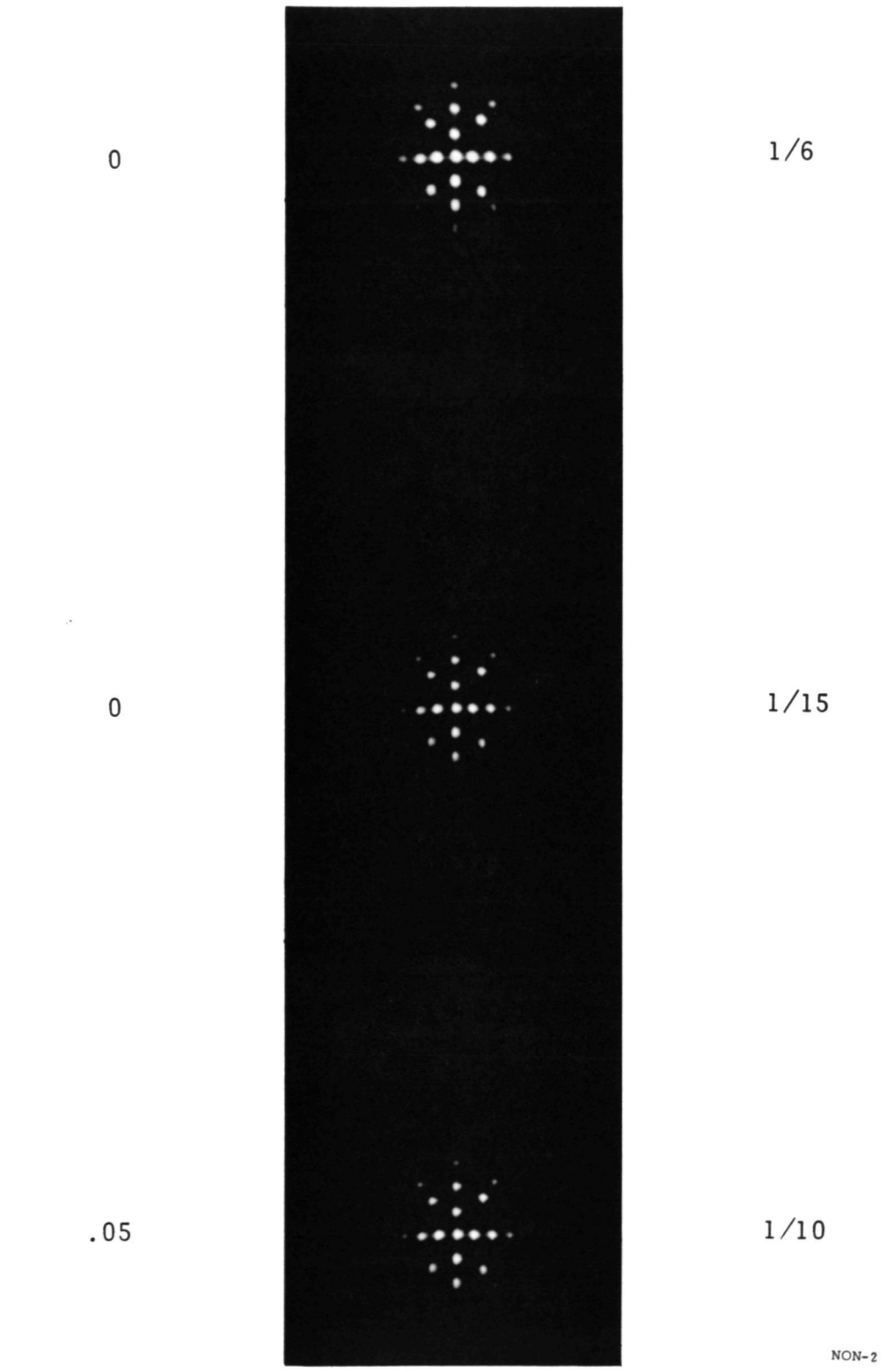

Figure 2-5. Photographs of the Pinhole Array After the Realignment Performed Before the Second Flight.

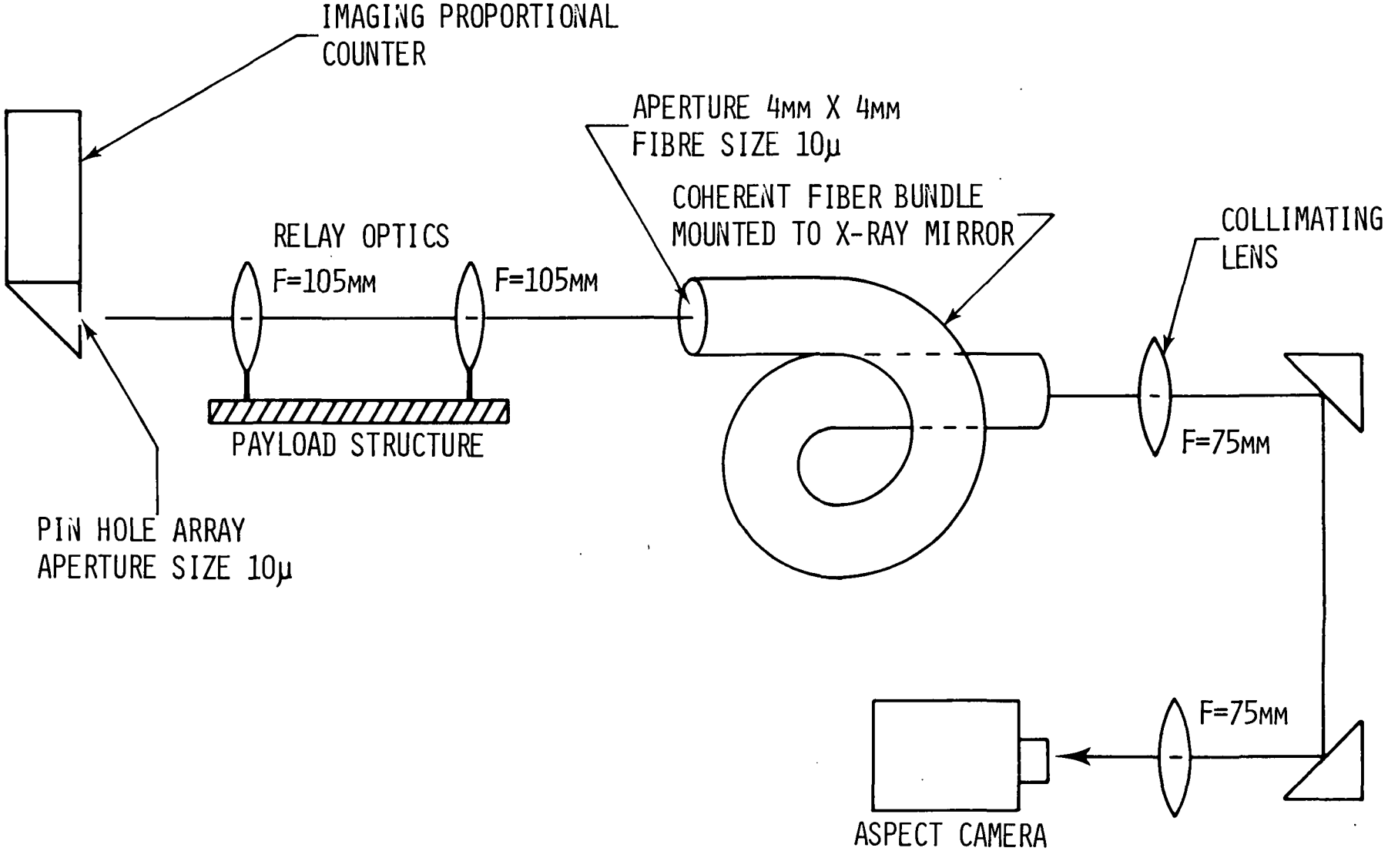

Figure 2-6. The Fiducial System

2.3 The Position Sensitive Detector

As described in Section 1.3 an Imaging Proportional counter was chosen for the detection device and the position sensing approach adopted was that of Borkowski and Kopp (1972). It consists of utilizing the cathode plane as an internal transmission line for signals that are induced by event signals in the anode plane. Charge produced by an x-ray interacting anywhere in the gas drifts along the parallel electric field toward the plane of the anode wires. Drift field electrodes, held several hundred volts above ground potential shape the field around the periphery of the active volume insuring that the electrons, liberated in the interaction, do not move laterally. Charge multiplication takes place at one of the wires in the anode plane as in a conventional proportional counter. Thus the anode signal contains information on the energy, absolute time of the original event and the pulse shape of the signal which can be used for discrimination against x-ray or particle events. For the present experiment the important fact is that the location of the event in the anode plane is preserved during the multiplication process and a localized signal is induced in each of the two orthogonally wound cathode planes. The cathode plane wire acts as a transmission line for the propagation of the signal from the point of maximum induced voltage to the ends of the wire. The transmission line is of the type where its characteristic time constant per unit length is large and the self-inductance and loss factor are small. Thus the rise time of the voltage signal arriving at the end of the wire depends on the length of transmission line the signal has traversed. By carefully choosing the composition of the wire and its diameter, a total resistance of several thousand ohms can be obtained and the resulting difference in rise time of the signal between the two ends of the wire determines the location of the induced signal to a precision of a few percent.

2.3.1 Design, Test and Operation

At the time of the transfer of affiliation of the Principal Investigator to the Smithsonian Astrophysical Observatory (SAO), it was mutually agreed that the development of the IPC should be undertaken by SAO. Consequently the development program will not be described in this report. For the flight counter, the external housing was designed by AS&E, while SAO was responsible for the design and internal arrangement of the electrodes. The focal plane assembly is shown in Figure 2-7 which shows the IPC surrounded by the pre-amplifier electronics and high voltage supplies and the gas supply system. Not shown is the vacuum door which protects the 1 micron polypropylene counter window during ground operations. It is needed because the counter , when using propane, is operated at half an atmosphere of pressure and the window is designed to withstand only outward directed pressures.

The prototype and flight counters were tested at AS&E using our soft X-ray vacuum facilities. Measurements of the position and energy resolution were made using pure propane and a mixture of 90% argon and 10% carbon dioxide as the proportional counter gases. In both respects propane proved to be superior and it was capable of providing one millimeter spatial resolution (corresponding to approximately 2 arc minute angular resolution with the rocket mirror) and adequate energy resolution at 0.28 keV. The position resolution improves with gain at the anode so the ultimate resolution is largely a function of the potential difference which can be sustained before breakdown occurs. This condition is determined by the surface condition of the anode wires. When breakdown does occur it was found that the anode plane was more susceptible to irreversible damage when propane was used. Consequently most of the test program was conducted with Argon-CO_2, although during the two flights propane was used.

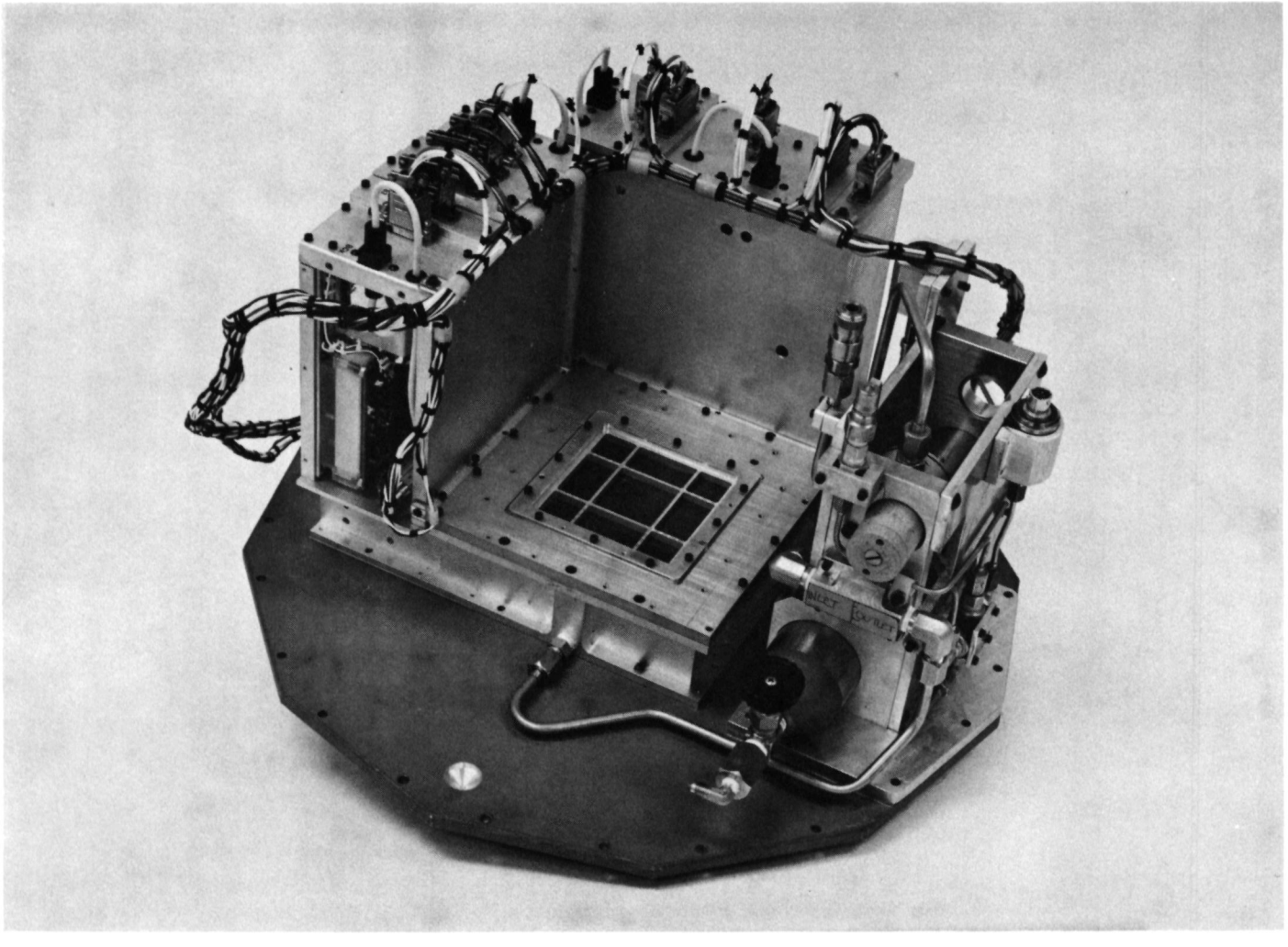

EW-047

Figure 2-7. Photograph of Focal Plane Assembly

The counter development program took considerably longer than had been initially anticipated and by the time a working prototype existed the technical specification of the counter-sampling electronics interface had undergone radical changes. So radical were the changes that the prototype electronics were quite unsuitable for operation with the counter. Consequently, as the test program had been run with standard rack mounted ORTEC modules it was decided to use similar units in the rocket payload. This required repackaging the ORTEC modules into the volume set aside for the processing electronics and providing the correct voltages and synchronizing signals.

2.3.2 Electronic Processing Circuits

Figure 2-8 is a schematic of the electronic processing system using the ORTEC modules. The circuits have 3 major functions. They are

(a) determine the position co-ordinates of each event

(b) measure the incident energy of the photons producing the events recorded in (a) above.

(c) discriminate against γ- ray and particle induced events.

Of these only the first presents any serious design problems and in the present application circuits from the earlier one dimensional focusing payload were modified to perform the pulse height analysis and anti-coincidence functions. The position sensing circuits operate as follows. Signals induced by an electron avalanche at the anode are detected and amplified by non-inverting pre-amplifiers connected to both ends of the cathode. The signals have rise times between a few tens and a few hundred nanoseconds depending upon the location of their origin along the cathode (See Figure 2-9 for a pictorial representation of the pulse shapes). The rise time, t_r, of the pulse is measured from a selected threshold to the point of inflection occurring on the leading edge of the voltage

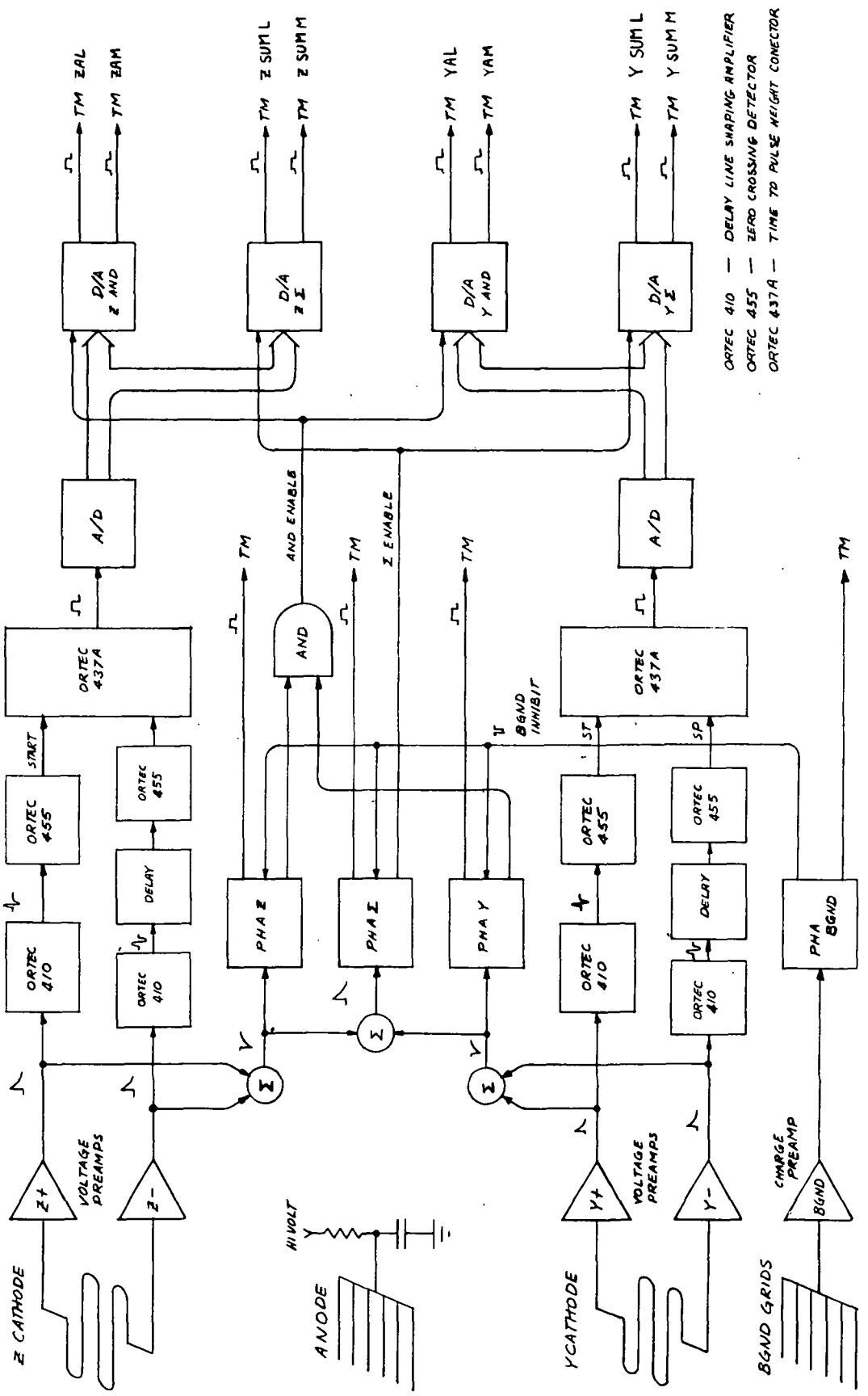

Figure 2-8. Simplified Block Diagram of the Data Processing Circuits.

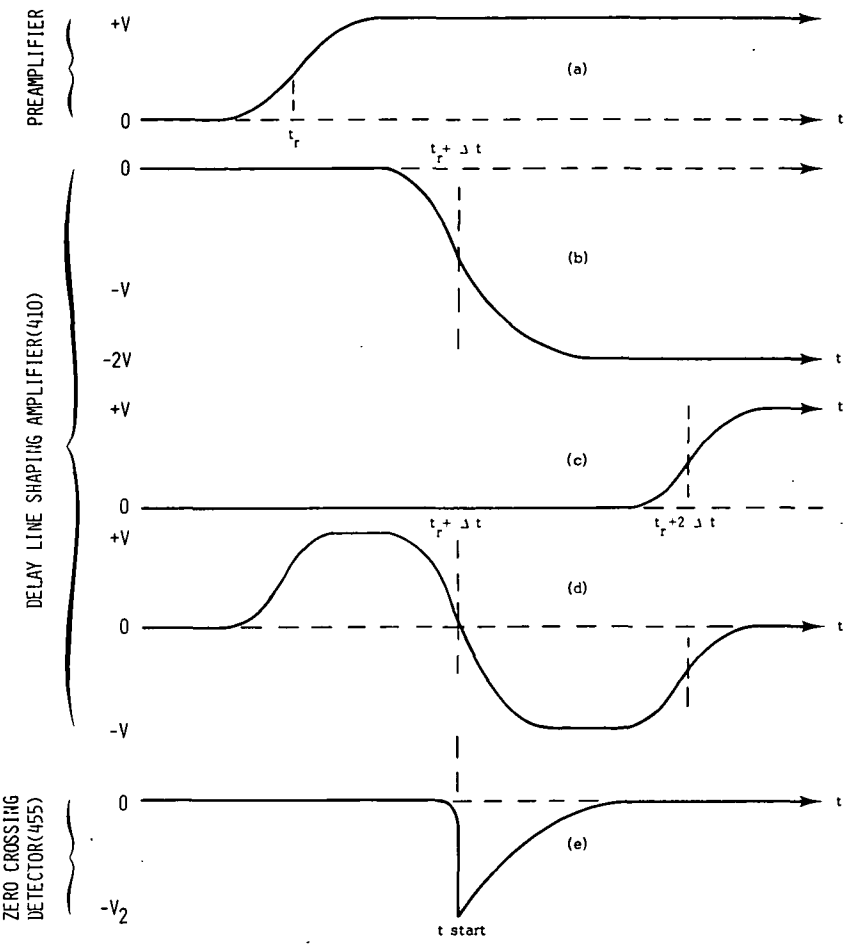

Figure 2-9 Pulse Shapes and Times for a Single Cathode

(a) The preamplifier output showing the position of the inflection point, t_r, which defines the pulse rise time .

(b) The preamplifier pulse is delayed by a time Δt, inverted and amplified by factor 2.

(c) The preamplifier pulse is delayed by a time $2\Delta t$, without amplification.

(d) Pulses (a), (b), and (c) are added to form a bipolar pulse whose zero-crossing occurs at $t_r + \Delta t$.

(e) The output of the zero-crossing detector which provides the start pulse for the 437A.

pulse. This is the point where the slope of the leading edge is steepest. Consequently, if we consider the signal to be the composition of the true signal, v, plus a constant noise component $\pm \delta v$, the effect of the noise on the voltage signal, resolved into an uncertainty in time, will be a minimum when the slope is a maximum. To define this time electronically the pulse is shaped using delay line clipping and amplification in the ORTEC 410 unit (Figure 2-9). The output from the 410 is a bipolar pulse and the point of inflection of the original pulse is now defined by the time of zero-crossing. It occurs at time $t_r + \Delta t$ where Δt is a delay time introduced in the shaping process. The zero crossing is detected by the ORTEC 455 operated in the bipolar mode. It generates a narrow pulse at the zero-crossing which is used to trigger the 437A, a time to height converter. Prior to the 455, pulses from both ends of the cathode are treated identically. However since either pulse can suffer the greater rise time delay in order to measure the difference an additional delay (set equal to the total cathode delay) is introduced in one channel. The undelayed pulse is used to trigger the 437A and start the timing pulse and the delayed pulse to end it. Thus the measured delay can vary from zero to twice the total cathode delay and the position of the event along the cathode is proportional to the difference in rise times between the pulses detected at the opposite ends of the cathode. If no stop signal is received within a fixed time the 437A is reset. The output from the 437A is digitized in an 8 bit analog to digital converter. The eight bits are separated into the 4 least and the 4 most significant before entry into digital to analog converters. The separation is necessary as 16 is a practical maximum for the number of levels which can be unambiguously defined within a single telemetry

channel. In the final digital to analog converters, the data pulses are stretched, and if the real event criteria are satisfied displayed to the telemetry interface for approximately 1.5 msec or slightly longer than twice the sampling frequency.

Two criteria for classifying real events have been developed which are identified as SUM and AND. In the SUM mode the pulse amplitude resulting from the linear summation of all four preamplifier outputs must exceed a certain threshold. This acceptance criterion is based on the total charge of the event. When it is satisfied cathode position and the summed preamplifier outputs are displayed to telemetry.

The second or AND mode requires that the linear sum of both the Y and Z preamplifiers, considered separately, must exceed specific thresholds. For this case the cathode position and the separate preamplifier summed outputs are transmitted.

Signals from the background wires are used to detect γ-rays and particles traversing the counter and the presence of a background signal in coincidence with either the SUM or AND signals overrides the acceptance criteria.

In the first flight (17.015UG) two pulse position modulation (PPM) transmitters were used to provide redundancy and the channel assignments are shown in Table II. In addition to the scientific data, aspect camera information and housekeeping functions are also transmitted.

For the second flight (17.016UH) the telemetry interface and processing system was redesigned to take advantage of the pulse coded modulation (PCM) telemetry which was now available. At the same time it was possible to eliminate quantizing problems

TABLE II

17.015UG TELEMETRY CHANNEL ALLOCATION

CHANNEL	PPM #1, 232.9 MHz	PPM #2, 244.3 MHz
2	Y sum L	YAL
3	Y sum M	YAM
4	Z sum L	ZAL
5	Z sum M	ZAM
6	PY	P sum
7	PZ	PB
8	Commutator Pole 2	Commutator Pole 1
9	Coding Light	Shutter
10	Y sum L	YAL
11	Y sum M	YAM
12	Z sum L	ZAL
13	Z sum M	ZAM
14	PY	P sum
15	PZ	PB
16	Clutch	Clock

Note: Channels 2&10, 3&11, 4&12, 5&13, 6&14, 7&15, tied together in experiment

Legend

1. Y refers to the proportional counter Y cathode
2. Z refers to the proportional counter Z cathode
3. Sum refers to the SUM logic coincidence condition
4. A refers to the AND logic coincidence condition
5. L and M refer to the least and most significant bits
6. P refers to pulse height data
7. B refers to data from the counter background wires
8. The commutator assignments are shown in Table III.

TABLE III

COMMUTATOR ASSIGNMENTS

FOR 17.015UG

SEGMENT	FUNCTION - POLE 1	FUNCTION - POLE 2
1	+5V	+5V
2	+5V	+5V
3	+5V	+5V
4	Low Pressure - Course	Low Pressure - Course
5	Low Pressure - Fine	Low Pressure - Fine
6	4.0V	4.0V
7	3.0V	3.0V
8	2.0V	2.0V
9	1.0V	1.0V
10	GND	GND
11	+ 28.5V Power IN	+30V, - 28.5V Y OUT
12	+ 28.5V Power OUT	EXT-INT Position
13	Camera Timed Power	Vacuum Chamber Door
14	HVPS Timed Power	Fiducial Light #1
15	Time Delay Relay Power	Fiducial Light #2
16	HVPS Input Power #1	± 16.5V Power IN
17	HVPS Input Power #2	+ 9V Power IN
18	Squib Battery 1&2-Armed	+30V, - 28.5V Power IN
19	Squib Mon #1	Clutch Pulse
20	Squib Mon #2	Clutch Pulse
21	Not Used	+30V, - 28.5V Z OUT
22	HVPS-Anode	+9V #1 Power OUT
23	HVPS-Z Cathode	+9V #2 Power OUT
24	HVPS-Y Cathode	± 12V Regulator
25	HVPS-Background	+16.5V Preamp Power OUT
26	± 16.5V Logic Pwr OUT	±16.5V Logic Pwr OUT
27	± 16.5V Logic Pwr OUT	±16.5V Logic Pwr OUT
28	± 16.5V Preamp Pwr OUT	High Pressure
29	± 16.5V Preamp Pwr OUT	Temperature
30	+5V	Clutch Pulse

that had resulted from the digitizing of the data for display to the telemetry. The basic concept is shown in Figure 2-10. The selection criteria of the SUM and AND modes are the same as in the earlier design and are tested in the amplifier/discriminator. In the SUM mode, the discriminator output drives the SUM timing control logic where control signals are generated for three sample and hold display elements. These sample the 437A outputs and the amplitude of the summed preamplifier outputs. After stretching the samples are displayed to the telemetry interface for 1.5 msec.

In the AND mode, a coincidence is required between Y and Z discriminator outputs to initiate sampling and display. In this case no pulse height information is recorded. The channel assignments are shown in Table IV.

2.3.3 Circuit Diagrams

A complete set of circuit diagrams, including printed circuit board layouts of

(i) the electronic data processing system and telemetry interface,

(ii) the control system, harnesses and housekeeping,

and (iii) the ground support equipment,

were prepared during the design, fabrication and test phases of the contract. Although not included in this report they are available upon request.

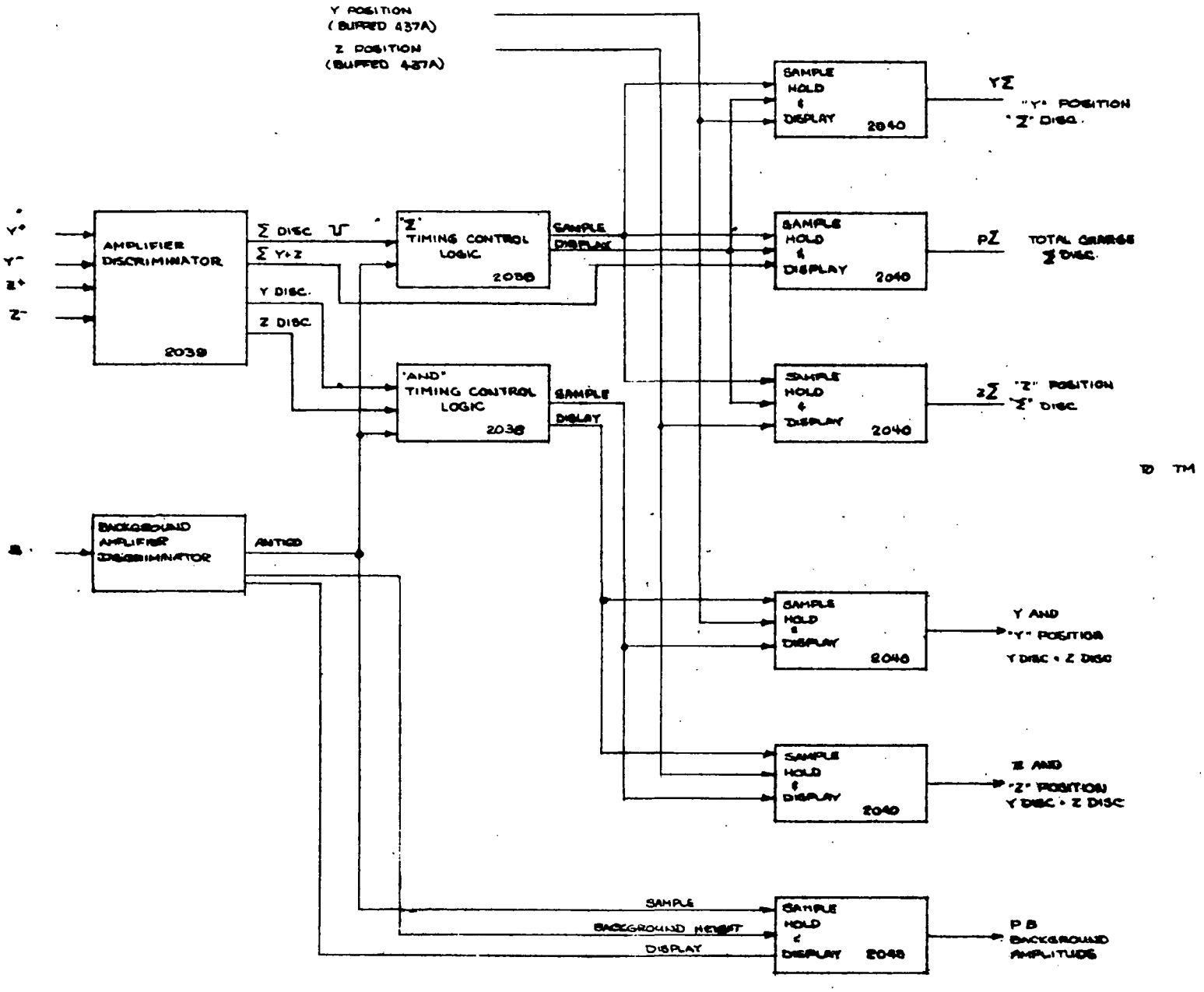

Figure 2-10. Block Diagram of the Modified Telemetry Interface for the PCM System.

TABLE IV

17.016 UH TELEMETRY CHANNEL ALLOCATION

CHANNEL	PCM #1, 232.9 MHz	PCM #2, 244.3 MHz
2	Y Sum	Y Sum
3	Z Sum	Z Sum
4	YA	YA
5	ZA	ZA
6	P Sum	P Sum
7	PB	PB
8	Clock	Clock
9	Coding Light	Shutter
10	Y Sum	Y Sum
11	Z Sum	Z Sum
12	YA	YA
13	ZA	ZA
14	P Sum	P Sum
15	Clutch	Clutch

Note: Channels 2 & 10, 3 & 11, 4 & 12, 5 & 13, 6 & 14 tied together in experiment.

Legend

1. Y refers to the proportional counter Y cathode
2. Z refers to the proportional counter Z cathode
3. Sum refers to the SUM logic coincidence condition
4. A refers to the AND logic coincidence condition
6. P refers to pulse height data
7. B refers to data from the counter background wires
8. Housekeeping Data Transmitted on a separate FM/FM Transmitter.

3.0 FLIGHT OPERATIONS FOR 17.015UG and 17.016UH

3.1 17.015UG

Following fabrication of the payload an extensive testing program was undertaken to demonstrate the integrity of the instrument. The program included separate vibration tests of the electronics panel to show that the repackaged ORTEC units would survive the launch environment. The test program was completed in early December, 1974 and following a successful systems test the payload was shipped to GSFC for integration which ran between 9 and 20 December, 1974.

The major events included the integration of the star tracker and its co-alignment to the payload optical axis. Following the vibration of the complete payload at proto-flight levels, the alignment was rechecked and was found to have remained aligned to within 10 arc minutes. In order to balance the payload it was necessary to add 4.1kg of ballast divided between the nose and parachute container. No serious problems were experienced with the electrical operation of the payload prior to or following T and E and it was returned to AS&E for a final calibration before shipping to White Sands.

During the calibration period, the IPC and signal electronics were adjusted for best operation using the soft x-ray vacuum facility at AS&E. When the Principal Investigator was satisfied with its performance the payload was shipped to White Sands.

Field operations for 17.015UG, which commenced on 26 February, 1975, were not uneventful as serious problems were experienced with the IPC window, which developed leaks and had to be replaced, necessitating a second set of final calibrations and with a failure of the aspect camera. The problems were all solved and the payload was placed in the tower and the vertical test held on 7 March. The

launch was scheduled for 10 March, but owing to high winds the launch was cancelled and rescheduled for 14 March. The winds were slightly lower on this night and the launch occurred at the end of the evening's window. The rocket described a perfect trajectory and all the instrument systems operated correctly. Unfortunately it was discovered that the star tracker had failed to acquire the targets correctly. That is they had been acquired but with large offsets that placed them at the edge of the field of view. However the final target, the Crab nebula, which was to be used as an inflight calibration source was seen and clearly demonstrated that the detector was position sensitive.

The payload was recovered successfully with only slight damage to the x-ray mirror.

3.2 17.016UH

Following the flight of 17.015UG which had demonstrated that the instrument was operational but had failed to return any significant data a reflight was authorized. The refurbishment included cleaning the mirror and modifying the telemetry interface as described in Section 2.3.2.

When the mirror was washed to remove the dirt which had adhered to the plates on impact, it was found that the gold coating was poorly bonded to the glass and in the majority of plates the metal coatings were stripped away. Consequently it was necessary to have the plates recoated and to completely realign the x-ray mirror. However after recoating and realignment the optical performance of the mirror was considerably improved (Section 2.2.2)

The redesign of the telemetry interface simplified the IPC testing procedures and a considerable effort was expended in optimizing the counter performance.

The payload underwent integration at GSFC between 6 and 14 November, 1975. No serious problems were experienced and the payload was shipped directly to White Sands.

Field Operations started on 24 November, and apart from a problem with the counter gas system the operations went according to schedule. The payload was placed in the tower on 3 December and launched on the night of 5 December, 1975. The flight was a complete success and excellent scientific data were obtained on the Perseus cluster and the Crab Nebula.

4.0 CONCLUSIONS

Contract NASW-2292 had been issued to support a program whose objectives were to obtain two dimensional images of stellar x-ray objects. It required the development of two new scientific instruments. - a large area x-ray focusing collector with arc minute resolution and a position sensitive detector capable of operating in the soft x-ray region (0.25 to 5 keV). The instruments were developed and in both cases, the original design criteria were either attained or exceeded. The instruments were combined into a sounding rocket payload which functioned correctly on the two flight opportunities that were available.

The second flight, 17.016UH, was completely successful and it obtained the first true images of the Crab Nebula and the Perseus Cluster thus demonstrating unequivocally the operation of the instrumentation and the achievement of the scientific objectives specified in the contract.

5.0 PERSONNEL AND ACKNOWLEDGEMENTS

The success of the Sounding Rocket program described in this report has been the result of the efforts of many individuals. In particular Al DeCaprio was in charge of the structural design and manufacture of the payload and the x-ray mirror assembly. Joseph Ting and Heinz Manko were responsible for the electrical design of the housekeeping and data processing circuits respectively. The development of the IPC was undertaken by Dr. Rick Harnden, first at AS&E and later at the Center for Astrophysics. Robert Rasche, of Measurement Laboratories, Inc., has acted as an electrical engineering consultant and participated in both field trips. He was instrumental in optimizing the data processing circuitry. At AS&E the program has been managed by Dr. John Davis, working under the direction of the Principal Investigator, Dr. Paul Gorenstein of the Smithsonian Astrophysical Observatory.

We would like to thank all the personnel of the Sounding Rocket Division of GSFC and the staff at the White Sands Missile Range who assisted in the integration and launch of the payloads.

Finally we would like to acknowledge the help of Mr. John Guidotti of the Sounding Rocket Division of GSFC who has provided consistent help and support for the program.

REFERENCES

Borkowski C.J. and M.K. Kopp, A Proportional Counter Photon Camera, I.E.E. Trans. on Nuc. Sci., NS-19, No. 3, 161, 1972.

Charpak, G. High Accuracy Position Measurements with Drift Chambers and Proportional Counters, I.E.E. Trans. on Nuc. Sci., NS-21, No. 1, 38, 1974.

Giacconi, R and B. Rossi, A Telescope for Soft X-ray Astronomy, J. Geophys. Res., 65, 773, 1960.

Gorenstein, P., B. Harris, H. Gursky and R. Giacconi, A Rocket Payload Using Focusing X-ray Optics for the Observation of Soft Cosmic X-rays, Nucl. Instr. and Methods, 91, 451, 1971.

Gorenstein, P., DeCaprio, A., Chase, R., and Harris, B., Large Area Focusing Collector for the Observation of Cosmic X-Rays, Rev. Sci. Instr., 44, 539, 1973.

Kirkpatrick, P. and A.V. Baez, Formation of Optical Images by X-rays, J. Opt. Soc. Am., 38, 766, 1948.

Perez-Mendez, V. and S.I. Parker, Recent Developments in Delay Wire Readout of Multiwire Proportional Chambers, I.E.E. Trans. on Nuc. Sci., NS-21, No. 1, 45, 1974.

Vaiana, G.S., Methods of Imaging X-ray Astronomy, CNES Space Optics, Marseilles, Gordon & Breach, New York, 295, 1970.

Van Speybroeck, L.P., R.C. Chase and T.F. Zehnpjennig, Orthogonal Mirror Telescopes for X-ray Astronomy, Applied Optics, 10, 945, 1971.

Wolter, H., Glancing Incidence Mirror Systems as Imaging Optics for X-rays, Ann. Physik., 10, 94, 1952a.

Wolter, H., A Generalized Schwarzschild Mirror System for Use at Glancing Incidence for X-ray Imaging, Ann. Physik, 10, 286, 1952b.